Comparisons of Elasto-Fiber and Fiber & Bernoulli-Euler reinforced concrete beam-column elements

Muhammet Karaton[*]

Civil Engineering Department, Engineering Faculty, Fırat University, 23119, Elazig, Turkey

Abstract.   In this study, two beam-column elements based on the Elasto-Fiber element theory for reinforced concrete (RC) element have been developed and compared with each other. The first element is based on Elasto Fiber Approach (EFA) was initially developed for steel structures and this theory was applied for RC element in there and the second element is called as Fiber & Bernoulli-Euler element approach (FBEA). In this element, Cubic Hermitian polynomials are used for obtaining stiffness matrix. The beams or columns element in both approaches are divided into a sub-element called the segment for obtaining element stiffness matrix. The internal freedoms of this segment are dynamically condensed to the external freedoms at the ends of the element by using a dynamic substructure technique. Thus, nonlinear dynamic analysis of high RC building can be obtained within short times. In addition to, external loads of the segment are assumed to be distributed along to element. Therefore, damages can be taken account of along to element and redistributions of the loading for solutions. Bossak-α integration with predicted-corrected method is used for the nonlinear seismic analysis of RC frames. For numerical application, seismic damage analyses for a 4-story frame and an 8-story RC frame with soft-story are obtained to comparisons of RC element according to both approaches. Damages evaluation and propagation in the frame elements are studied and response quantities from obtained both approaches are investigated in the detail.

Keywords: Elasto-Fiber element; Fiber & Bernoulli-Euler element; seismic damage analysis; dynamic substructure technique; Bossak-α method and predicted-corrected method

1. Introduction

In the last thirty years, researchers have made more effort for the numerical modeling of reinforced concrete (RC) structures and most of the state-of-the-art on this problem deals with two main approaches; lumped plasticity modeling (Anagnostoupoulos 1981, Banon *et al.* 1981, Zeris and Mahin 1991, Isobe and Tsuda 2003) and distributed-inelasticity modeling (i.e., the so-called Fibre beam-column elements, FBCE) (Filippou and Issa 1988, Taucer *et al.* 1991, Carlson 1999, Li Y *et al.* 2011, http://opensees.berkeley.edu). In the first approach, nonlinear springs based on moment-rotation and force-displacement curves are used and nonlinear volume is assumed to be lumped in the specific location of the element (Anagnostoupoulos 1981, Banon *et al.* 1981, Zeris and Mahin 1991). In the second approach, the nonlinear behaviors of concrete and reinforcement

---

[*]Corresponding author, Assistant Professor, E-mail: mkaraton@firat.edu.tr

materials are separately calculated. This method is divided into two as approaches based on flexibility and rigidity. Taucer *et al.* (1991), developed a flexibility method for nonlinear dynamic analysis of reinforced concrete element. This method, based on Bernoulli-Euler hypothesis, includes biaxial bending and axial force conditions. Nonlinear behavior of concrete and steel are computed by using their uniaxial stress-strain relationships. Force-displacement interpolation functions are used for obtaining the element flexibility matrix. Element stiffness matrix is computed by inverse of flexibility matrix. Furthermore, Kawano *et al.* (1998), Ceresa *et al.* (2009), Lu *et al.* (2013) investigated the shear effect on reinforced concrete element. The methods based on rigidity are not preferred generally due to flexural deformation of RC element in intensity damage regions (Kawano *et al.* 1998). In the last time, the strain rate effects on response of reinforced concrete frames were investigated by Iribarren (2010). Formulation based on rigidity method is used for the solutions and a strain rate dependent material formulation was developed for both the concrete and steel constitutive response. Karaton (2013) used a method based on rigidity for nonlinear dynamic analysis of RC frames. A nonlinear dynamic substructure technique was developed for eliminating of flexural deformation of RC element in intensity damage regions.

Elasto-Fiber Approach (EFA), used in this study was firstly developed for steel structures by Krishnan (2003). In the EFA based on rigidity, beam or column element was divided into sub-elements called "segments". The segment freedoms at internal region of the element were condensed by using static substructure technique to segment freedoms at the end of the element. Thus, nonlinear dynamic analysis of high steel building can be obtained within short time (Krishnan 2003). This procedure requires nested loops of the element and structure that are obtained at the same time. But, external loads at internal element regions are lumped to ends of the element. These loads are not included in the element iterative solutions and redistribution of the element external loads is not taken into account due to the problem arising in the numerical solutions. Therefore, the redistribution of loads must be calculated for more realistic solutions of RC frames and the numerical problem must be overcome.

Cubic Hermitian polynomials in Fiber&Bernoulli-Euler element approach (FBEA) are used for obtaining stiffness matrix and these polynomials are not sufficient due to flexural deformation of reinforced concrete material in heavy damage regions. Therefore, FBEA is not preferred for analyses of the RC structures (Kawano *et al.* 1998). A dynamic substructure technique for FBEA was applied by Karaton (2013) for eliminating to the disadvantage of Cubic Hermitian polynomials. In this research, numerical results with experimental results of a reinforced concrete column are compared and effectiveness of the approach is investigated in details.

The present research has been organized as (*i*) obtaining of constitutive models for RC frames according to EFA and FBEA, (*ii*) developing of nonlinear dynamic substructure technique for EFA and FBEA, (*iii*) applying of Bossak-α method for the nonlinear dynamic analysis of frames, (*iv*) obtaining of seismic damage analyses for a 4-story frame and an 8-story RC frame with soft-story and comparing of the responses for both approaches and (*v*) results.

2. EFA and FBEA for reinforced concrete beam-column elements

2.1 Obtaining element stiffness matrices for EFA

The strain distribution on a cross section of the beam is assumed to be uniform due to only axial forces and linear due to only bending according to the Bernoulli-Euler approach (Carlson

1999, Krishnan 2003, Lu *et al*. 2013, Karaton 2013). Furthermore, if a section is plane before bending, it is plane after bending and if the strain is assumed to be small, the incremental strain of a point on a cross-section in the axial direction can be written as

$$d\varepsilon_{\xi,n} = \frac{du_j - du_i}{L_{seg}} + \frac{\eta_n'(d\phi_{j,\zeta} - d\phi_{i,\zeta})}{L_{seg}} \tag{1}$$

where du_i and du_j are the displacements of i and j ends of the a segment in the ξ (axial) direction, respectively. $d\phi_{i,\zeta}$ and $d\phi_{j,\zeta}$ are rotations of i and j ends of the a segment at about ζ axis, respectively. L_{seg} is segment length and η' is also coordinate of a fiber/layer in η axis direction (Fig. 1). Thus, incremental normal stress of a fiber/layer in the ξ axis direction can be defined as

$$d\sigma_{\xi,n} = E_{T,n} d\varepsilon_{\xi,n} \tag{2}$$

where, $E_{T,n}$ is tangent elasticity modulus of nth fiber. Thus, axial force, P_ξ and total bending moment, M_ζ are obtained as

$$P_\xi = \sum_{n=1}^{nfib} E_{T,n} A_n \tag{3.a}$$

$$M_\zeta = \sum_{n=1}^{nfib} E_{T,n} A_n \eta_n' \tag{3.b}$$

where, A_n is area of nth fiber. Furthermore, the internal shear forces, Q_η by using elasticity theory and material properties of the cross-section are defined as

$$Q_\eta = -\sum_{n=1}^{nfib} G_{T,n} A_{s,n} \phi_\zeta \tag{4}$$

where, $A_{s,n}$ and $G_{T,n}$ is shear area and tangent shear modulus of nth fiber, respectively. ϕ_ζ is also rotation of the cross section relative to the chord. $G_{T,n}$ is obtained by using tangent elasticity module and Poisson ratio of the material. In Eq. (4), if shear strain is assumed constant as along the element to prevent to shear locking, shear forces by using rotations at i and j ends of element can be expressed as

$$Q_\eta = -\sum_{n=1}^{nfib} G_{T,n} A_{s,n} \frac{\phi_{i,\zeta} + \phi_{j,\zeta}}{2} \tag{5}$$

Therefore, Elasto-Fiber element theory is modified by using Eq. (5) for section with the reinforced concrete (or composite). Incremental forms of Eqs. (3) and (5) can be written as

$$dP_\xi = \sum_{n=1}^{nfib} E_{T,n} A_n d\varepsilon_{\xi,n} \tag{6.a}$$

$$dM_\zeta = \sum_{n=1}^{nfib} E_{T,n} A_n \eta_n' d\varepsilon_{\xi,n} \tag{6.b}$$

$$dQ_\eta = -\sum_{n=1}^{nfib} G_{T,n} A_{s,n} \frac{d\phi_{i,\zeta} + d\phi_{j,\zeta}}{2} \qquad (6.c)$$

These incremental relations in the matrix form, by using Eqs. (1) and (2), can be rewritten as

$$\begin{Bmatrix} dP_\xi \\ dM_\zeta \\ dQ_\eta \end{Bmatrix} = \frac{1}{L_{seg}} \begin{bmatrix} \sum_{n=1}^{nfib} E_{T,n} A_n & -\sum_{n=1}^{nfib} E_{T,n} A_n \eta_n' & 0 \\ -\sum_{n=1}^{nfib} E_{T,n} A_n \eta_n' & \sum_{n=1}^{nfib} E_{T,n} A_n (\eta_n')^2 & 0 \\ 0 & 0 & \sum_{n=1}^{N} G_{T,n} A_{s,n} \end{bmatrix} \begin{Bmatrix} du_j - du_i \\ -(d\phi_{j,\zeta} - d\phi_{i,\zeta}) \\ -\frac{(d\phi_{i,\zeta} + d\phi_{j,\zeta})}{2} L_{seg} \end{Bmatrix} \qquad (7.a)$$

or

$$\{dF\} = [C_T]\{B\} \qquad (7.b)$$

The $\{B\}$, vector for displacements and rotations of i and j ends of the segment can be rearranged as follow

$$\begin{Bmatrix} du_j - du_i \\ -(d\phi_{j,\zeta} - d\phi_{i,\zeta}) \\ -\frac{(d\phi_{i,\zeta} + d\phi_{j,\zeta})}{2} L_{seg,n} \end{Bmatrix} = \begin{bmatrix} -1 & 0 & 0 & 1 & 0 & 0 \\ 0 & 0 & 1 & 0 & 0 & -1 \\ 0 & -1 & \frac{L_{seg,n}}{2} & 0 & 1 & \frac{L_{seg,n}}{2} \end{bmatrix} \begin{Bmatrix} du_i \\ dv_i \\ d\phi_{i,\zeta} \\ du_j \\ dv_j \\ d\phi_{j,\zeta} \end{Bmatrix} \qquad (8.a)$$

or

$$\{B\} = [S]\{dU\} \qquad (8.b)$$

Thus, segment tangent stiffness matrix, by using minimum potential energy principle, is obtained as the following

$$[K]_{seg} = \frac{1}{L_{seg,n}} [S]^T [C_T][S] \qquad (9)$$

The segment stiffness matrix is obtained by using areas, coordinates and tangent elasticity modulus of each fiber/layer (concrete/reinforcement) in each segment. Tangent elasticity modulus of each concrete/reinforcement can be calculated by using uniaxial stress-strain relationship of each material and linear superposition rule is used for different fiber material properties in the
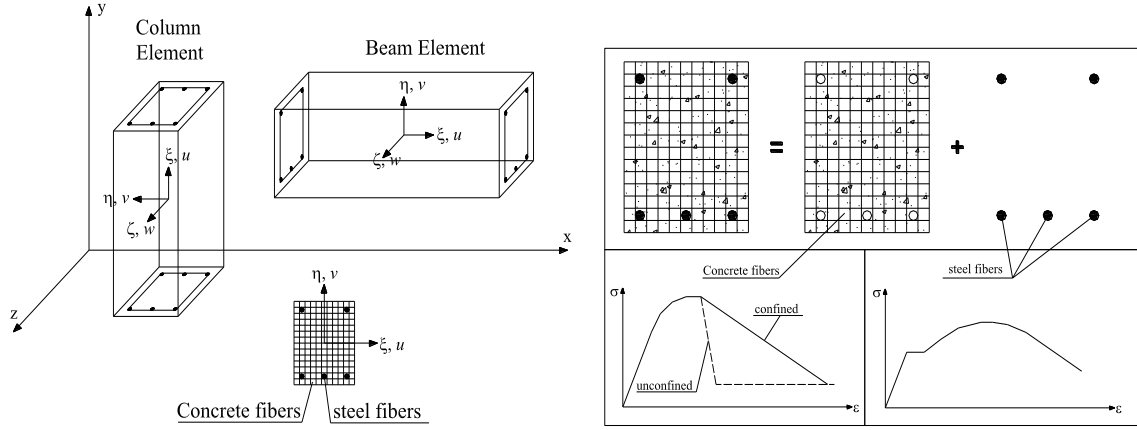
Fig. 1 Concrete, steel fibers and global and local axis

section (Fig. 1). However, concrete/reinforcement fibers may be damaged due to external loading and in order to obtaining a relationship between the damaged and undamaged case, damage intensity in each concrete and steel fiber is computed as follow (Légeron *et al*. 2005)

$$d_n = 1 - \frac{E_{T,n}}{E_{O,n}} \tag{10}$$

where, $E_{O,n}$ is undamaged elasticity module of nth fiber. d_n, damage intensities are separately obtained under tensile and compressive stress for each fiber. $E_{T,n}$, tangent elasticity module and $G_{T,n}$, tangent shear module of nth fiber by using damage intensity can be written as

$$E_{T,n} = (1 - d_n) E_{O,n} \tag{11.a}$$

$$G_{T,n} = (1 - d_n) G_{O,n} = (1 - d_n) \frac{E_{O,n}}{2(1 + v_n)} \tag{11.b}$$

However, total kinetic energy of particle velocities on the cross-section of an element throughout its neutral axis can be written as

$$T = \frac{1}{2} \int_\Omega v_\xi \rho v_\xi d\Omega \tag{12}$$

where, ρ is mass density and v_ξ is particle velocity in ξ, the axial direction (Fig. 1). If concrete/reinforcement fibers are used in Eq. (12), the mass matrices of an element on the local axis are obtained as

$$[M_{seg}] = \int_{-1}^{1} \sum_{n=1}^{nfib} \left([N(\xi)]^T \rho_n A_n [N(\xi)] \right) d\xi \tag{13}$$

where $[N(\xi)]$ is the element shape functions matrix and ρ_n is also mass density of nth fiber. Stiffness and mass matrices of a segment are transformed to global axes by using standard transformation matrix.
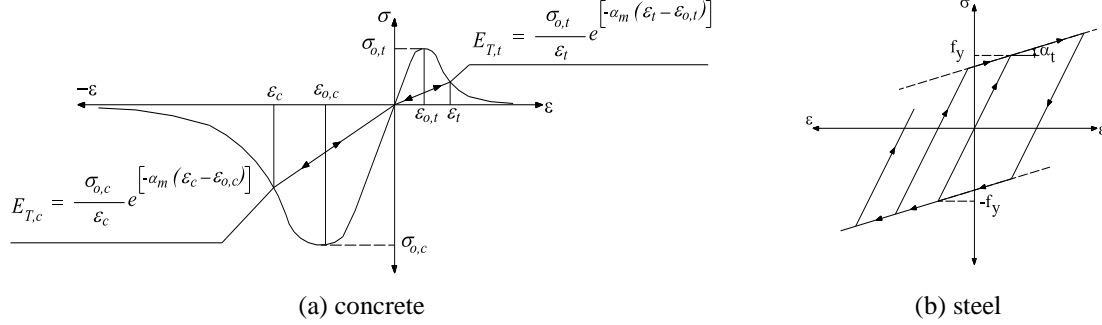
(a) concrete   (b) steel

Fig. 2 Stress-strain relationships for RC materials

2.2 Obtaining element stiffness matrices for FBEA

Differential form of Eq. (1), by using Bernoulli-Euler approach in the global axes, can be rewritten as

$$\varepsilon_{xx} = \frac{du}{dx} - \frac{d^2v}{dx^2} y \tag{14}$$

where u and v are the displacement of the axial and vertical directions of element, respectively (Fig. 1). However, if cross section of element is divided with concrete/reinforcement fibers, this equation for each concrete/reinforcement in local axis can be rewritten as

$$d\varepsilon_{\xi,n} = \left\{ l \quad -\eta_n' \right\} \begin{Bmatrix} du/d\xi \\ d^2v/d\xi^2 \end{Bmatrix} \tag{15}$$

where, $d\varepsilon_{\xi,n}$ is incremental axial strain of a fiber on a segment in ξ local axis direction. Therefore, if the cubic Hermitian polynomials for transversal displacements and the linear shape functions for axial displacements are used (Chandrupatla and Belegundu 2002), then the Eq. (2) can be written as

$$d\varepsilon_{\xi,n} = \left\{ l \quad -\eta_n' \right\} \begin{Bmatrix} d[N(\xi)]/d\xi \\ d^2[N(\xi)]/d\xi^2 \end{Bmatrix} \{q\} = \left\{ l \quad -\eta_n' \right\} [B]\{q\} \tag{16}$$

where, $\{q\}$ is displacement vector which include displacements and rotations of a segment. $[B]$ is strain-displacement matrix. Incremental stress in each concrete/reinforcement can obtained as,

$$d\sigma_{\xi,n} = E_{T,n} \, d\varepsilon_{\xi,n} = E_{T,n} \left\{ l \quad -\eta_n' \right\} [B]\{q\} \tag{17}$$

where, $E_{T,n}$ is determined by using uniaxial stress-strain relationship of each fiber. Total strain energy of a segment can be also achieved as

$$\Pi = \frac{1}{2} \int_{L_{Seg}} \sigma^T \varepsilon \, A_{Seg} \, d\, x = \frac{1}{2} \int_{-1}^{1} \{q\}^T [B]^T \left[\begin{Bmatrix} 1 \\ -\eta_n' \end{Bmatrix} E_{T,n} A \{1 \quad -\eta_n'\} \right] [B]\{q\} d\, \xi$$

$$= \frac{1}{2} \int_{-1}^{1} \{q\}^T [B]^T \begin{bmatrix} \displaystyle\sum_{n=1}^{N} E_{T,n} A_n & -\displaystyle\sum_{n=1}^{N} E_{T,n} A_n \eta_n' \\ -\displaystyle\sum_{n=1}^{N} E_{T,n} A_n \eta_n' & \displaystyle\sum_{n=1}^{N} E_{T,n} A_n \left(\eta_n'\right)^2 \end{bmatrix} [B]\{q\} d\, \xi \tag{18}$$

where, L_{Seg} and A_{Seg} are expressed to length and cross section area of segment, respectively. A_n is also area of a concrete/reinforcement fiber. Element stiffness matrix can be acquired by using minimum potential energy principle. The stiffness matrix of a segment can written as

$$[K_{Seg}] = \frac{1}{2} \int_{-1}^{1} [B]^T \begin{bmatrix} \displaystyle\sum_{n=1}^{N} E_{T,n} A_n & -\displaystyle\sum_{n=1}^{N} E_{T,n} A_n \eta_n' \\ -\displaystyle\sum_{n=1}^{N} E_{T,n} A_n \eta_n' & \displaystyle\sum_{n=1}^{N} E_{T,n} A_n \left(\eta_n'\right)^2 \end{bmatrix} [B] \, d\, \xi \tag{19}$$

In the FBEA, damages in each concrete/reinforcement fiber are calculated by using Eq. (10) and mass matrices of segment are obtained by using Eq. (13).

2.3 Nonlinear dynamic substructures technique for stiffness and mass matrices

The Gaus-Lobatto integration rule is generally used for obtaining element mass and stiffness matrices along to ξ local axis (Kawano *et al.* 1998, Ceresa *et al.* 2009, Iribarren 2010, Lu *et al.* 2013). The element stiffness matrix is obtained by using cross section properties on the integration points. Therefore, the effects of shape functions on the solution are very important. In the resent years, methods based on flexibility have been developed due to this disadvantage of methods based on rigidity for static and dynamic analyses of RC element. But, static or dynamic substructure procedures to eliminate this disadvantage of rigidity methods are generally not preferred due to numerical difficultly. Krishnan (2003) had used a static substructure technique for the nonlinear dynamic analysis of steel structure and arising problems due to flexural behavior of elements were removed. However, this substructure procedure is required to condensation to end freedoms at ends element of element external loads; in this case, redistribution of external loads is not taken into account. This redistribution must be computed in solution techniques.

In this study, a dynamic substructure technique is applied for the reinforced concrete frames. In this method, element is divided into segments and the freedoms of segment are condensed to the end freedoms at ends element. This procedure is used as the each element iteration in the iteration of frame structure. Freedoms at end and internal regions of element are called as external and internal freedoms, respectively (Fig. 3). The external and internal freedoms for stiffness matrices can be written as
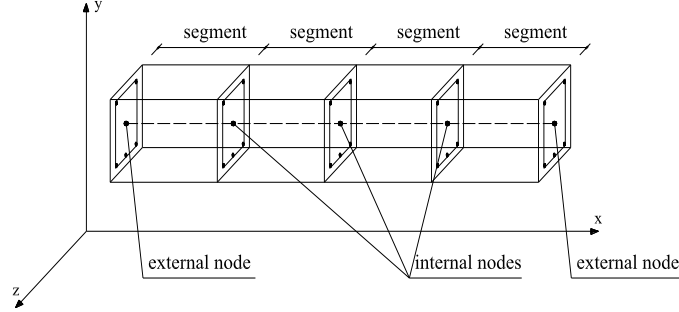
Fig. 3 Segments, external and internal nodes for EFA and FBEA

$$\begin{bmatrix} [K_{EE}] & [K_{EI}] \\ [K_{IE}] & [K_{II}] \end{bmatrix} \begin{Bmatrix} \{u_E\} \\ \{u_I\} \end{Bmatrix} = \begin{Bmatrix} \{F_E\} \\ \{F_I\} \end{Bmatrix} \qquad (20)$$

where, $[K_{EE}]$ and $[K_{II}]$ are stiffness matrices which include external and internal freedoms, respectively (Krishnan 2003). $\{u_E\}$ and $\{u_I\}$ are the displacement vectors referred by these freedoms. $\{F_E\}$ and $\{F_I\}$ are also the external loads belonging to these freedoms. If applying the substructure procedure for Eq. (20), the external load and stiffness matrices of a frame element can be rewritten as

$$[K_{EE,F}] \ \{u_E\} = \{F_{E,F}\} \qquad (21.a)$$

$$[K_{EE,F}] = [K_{EE}] - [K_{EI}] [K_{II}]^{-1} [K_{IE}] \qquad (21.b)$$

$$\{F_{E,F}\} = \{F_E\} - [K_{EI}][K_{II}]^{-1}\{F_I\} \qquad (21.c)$$

However, if the Rayleigh method is used for obtaining element damping matrices, the damping matrix is defined as

$$\begin{bmatrix} [C_{EE}] & [C_{EI}] \\ [C_{IE}] & [C_{II}] \end{bmatrix} = \alpha_{dam} \begin{bmatrix} [M_{EE}] & [M_{EI}] \\ [M_{IE}] & [M_{II}] \end{bmatrix} + \beta_{dam} \begin{bmatrix} [K_{EE}] & [K_{EI}] \\ [K_{IE}] & [K_{II}] \end{bmatrix} \qquad (22)$$

where α_{dam} and β_{dam} are Rayleigh damping coefficients, with respect to mass and stiffness matrices, respectively (Bathe 1982). However, if substructure procedure for mass and damping matrices (Guyan 1965) are applied, then the mass and damping matrices for external freedoms of element can be obtained as

$$[M_{EE,F}] = [M_{EE}] - [K_{EI}][K_{II}]^{-1}[M_{IE}] - [M_{EI}][K_{II}]^{-1}[K_{IE}] + [K_{EI}][K_{II}]^{-1}[M_{II}][K_{II}]^{-1}[K_{IE}] \quad (23a)$$

$$[C_{EE,F}] = [C_{EE}] - [K_{EI}][K_{II}]^{-1}[C_{IE}] - [C_{EI}][K_{II}]^{-1}[K_{IE}] + [K_{EI}][K_{II}]^{-1}[C_{II}][K_{II}]^{-1}[K_{IE}] \qquad (23b)$$

Global element stiffness, damping and mass matrices can be achieved and stiffness, damping, mass matrices and external load vector for the RC frames (or structure) can be calculated as

$$[K_S] = \sum_{k=1}^{nelem} [K_{EE,F}], \quad [C_S] = \sum_{k=1}^{nelem} [C_{EE,F}], \quad [M_S] = \sum_{k=1}^{nelem} [M_{EE,F}], \quad \{F_S\} = \sum_{k=1}^{nelem} \{F_{E,F}\} \qquad (24)$$

The dynamic equilibrium equation of the structure can be given as,

$$[M_S]\{a_E\}_{t+\Delta t} + [C_S]\{v_E\}_{t+\Delta t} + [K_S]\{u_E\}_{t+\Delta t} = \{F_{S,gr}\}_{t+\Delta t} + \{F_{S,stat}\} \qquad (25)$$

where subscript *gr* and *stat* indicate that the quantity is related with ground acceleration and static loads.

2.4 Bossak-α form of equation of motion

The equation of motion for the RC frame is given in Eq. (25). In this study, the Bossak-α integration method, presented by Wood *et al.* (1980), is used for the solution of the equation in the time domain and time integration scheme of the method retains the Newmark method. The Bossak-α integration method is required to be modified to Eq. (25) in the time domain as follows

$$(1-\alpha_B)[M_S]\{a_S\}_{t+\Delta t} + \alpha_B[M_S]\{a_S\}_t + [C_S]\{v_S\}_{t+\Delta t} + \{F_{S,res}\}_{t+\Delta t} =$$
$$(1-\alpha_B)\{F_{S,gr}\}_{t+\Delta t} + \alpha_B\{F_{S,gr}\}_t + \{F_{S,stat}\} \qquad (26)$$

where α_B is the Bossak parameter, used for controlling the numerical dissipation. The Bossak parameter should be chosen as in Eq. (27) for unconditional stability and second-order accuracy

$$\alpha_B \leq \frac{1}{2}; \qquad \beta = \frac{1}{4}(1-\alpha_B)^2; \qquad \gamma = \frac{1}{2} - \alpha_B \qquad (27)$$

In this study, α_B is selected as -0.10. To solve the non-linear dynamic equation of motion for the RC frame, the Newton-Raphson method is used in conjunction with the predictor-corrector technique. Predicted displacement and velocity vectors for the time step $t+\Delta t$ are obtained by using displacement and velocity vectors at the time step t, known. Thus, they can be calculated as

$$\{\tilde{u}_S\}_{t+\Delta t} = \{u_S\}_t + \Delta t\{v_S\}_t + \frac{1}{2}\Delta t^2(1-2\beta)\{a_S\}_{t+\Delta t} \qquad (28.a)$$

$$\{\tilde{v}_S\}_{t+\Delta t} = \{v_S\}_t + \Delta t(1-\gamma)\{a_S\}_t \qquad (28.b)$$

where β and γ are Newmark's coefficients. The displacement and velocity vectors (Miranda *et al.* 1989) of the RC frame can be written in terms of the predicted vectors shown in Eq. (28). The vectors can be defined as

$$\{u_S\}_{t+\Delta t} = \{\tilde{u}_S\}_{t+\Delta t} + \beta\Delta t^2\{a_S\}_{t+\Delta t} \qquad (29.a)$$

$$\{v_S\}_{t+\Delta t} = \{\tilde{v}_S\}_{t+\Delta t} + \Delta t\gamma\{a_S\}_{t+\Delta t} \qquad (29.b)$$

If these relations can be substituted into Eq. (26), a time marching algorithm can be applied as given in the Appendix.
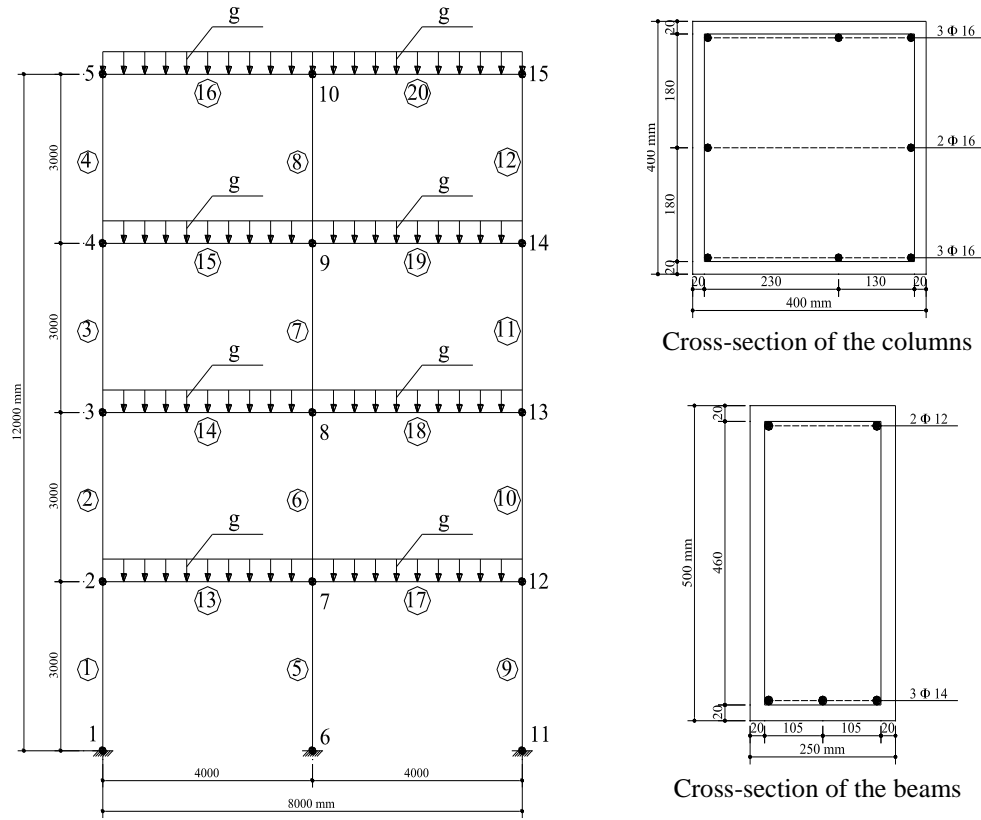
Fig. 4 Finite element mesh, columns and beams cross-section properties of 4-story frame
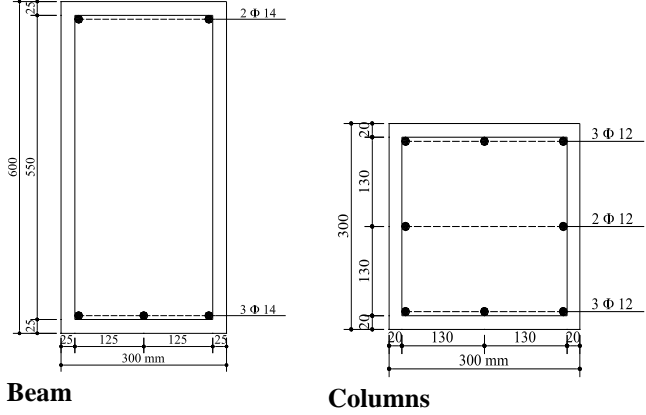
3. Numerical applications

Seismic damage analyses for 4-story and 8-story RC frame with soft-story are investigated for the comparison of EFA and FBEA. Comparisons of both approaches with each other are performed for response quantities, damages evaluation and propagation in these frames.

3.1 Nonlinear seismic analyses of a 4-story RC frame structure

In this subsection, nonlinear seismic analyses of 4-story RC frame are obtained according to the EFA and FBEA. Material and cross-section properties of the beam and column belong to the frame are given in Table 1 and the finite element mesh and loading case are shown in Fig. 4 for both approaches. ACI 318-02 (2002) code is used for the material properties of concrete and steel. Exponential decreasing functions are used for the softening region of tensile and compressive strengths of the concrete and the bilinear kinematic hardening behavior are selected for nonlinear behavior of the steel in the two approaches (Fig. 2). Static loads and element masses are assumed as distributed to the element along. Displacement values obtained due to the static loads are being considered as the initial condition. For the seismic effect, a target spectrum acceleration curve has been selected according to Z1 type soil in the Turkish Regulation on Building in Disaster Areas,

Table 1 Material and cross section properties of the portal frame example

		Beam	Columns
Concrete	Elasticity Mod. (E_c MPa)	25742.960	25742.960
	Comp. strength (f_c, MPa)	30.00	30.00
	Tensile strength (f_t, MPa)	2.74	2.74
	Mass density (ρ, ton/m^3)	2.4	2.4
	Poisson ratio[*]	0.15	0.15
Steel	Elasticity Modulus (E_s MPa)	210000	210000
	Yield strength (f_y, MPa)	420.0	420.0
	Tangent modulus (α_t)	0.05	0.05
	Mass density (ρ, ton/m^3)	7.951	7.951
	Poisson ratio[*]	0.30	0.30

[*]This material property is only used for EFA

TRBDA (2007) and a synthetic earthquake acceleration data has been produced by using the SeismoArtif program (http://www.seismosoft.com). Maximum amplitude of this acceleration data has been selected as 0.3 g. The time history graph of this synthetic acceleration data is shown in Fig. 5. This seismic load is applied to *x* (horizontal) direction of the frames. Nonlinear seismic analyses of the frame according to the both approaches are obtained by using damping with stiffness ratio.

Horizontal (*x*) and vertical (*y*) displacement time history graphs of node 5 obtained from the nonlinear seismic analyses of the FBEA and the EFA are shown in Fig. 6(a) and 6(b), respectively. Horizontal displacement time amplitude values are approximately similar until 1.20 sec. Furthermore, a small phase difference appears between both methods after the 1.20 sec. Absolute maximum displacement values for horizontal direction obtained from the EFA and the FBEA are 36.66 mm and 26.22 mm, respectively. Displacement amplitude values of the EFA are approximately 40% bigger than displacement values of the FBEA in horizontal direction. Vertical displacement values obtained from both approaches are similar until 1.20 sec. after this time, some different amplitude values are obtained for both approaches as horizontal displacement. Absolute maximum displacement values for vertical direction obtained according to the EFA and the FBEA are 0.49 mm and 0.42 mm, respectively. Absolute maximum displacement value of the EFA is approximately 17% bigger than the FBEA value in vertical direction. If these values are compared with horizontal displacement values, it may be seen that the said values were very small. These
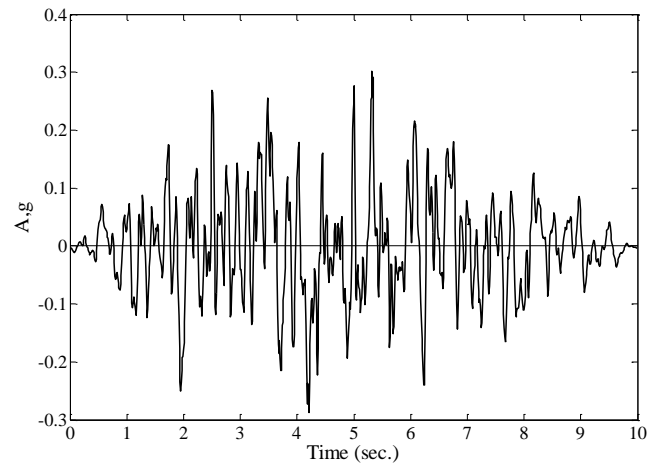
Muhammet Karaton

Fig. 5 Time history graphs of synthetic acceleration

(a) Horizontal

(b) Vertical
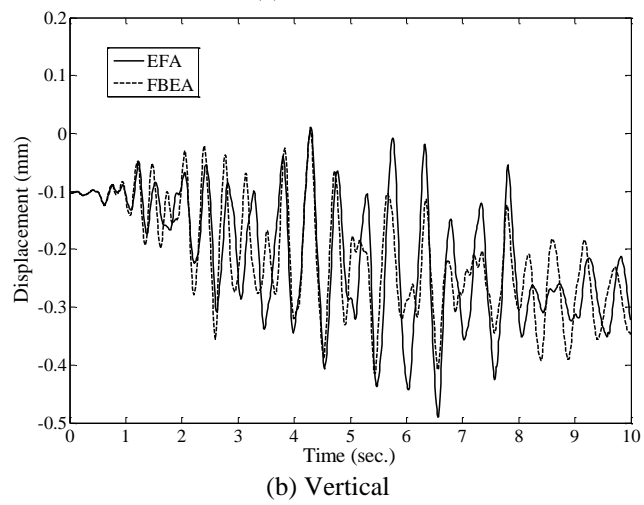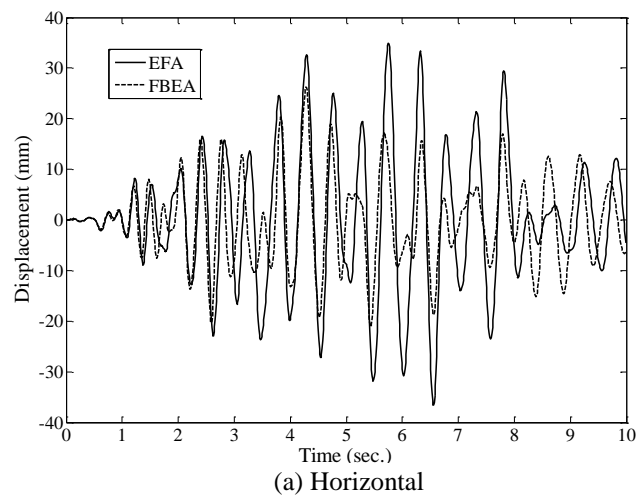
Fig. 6 Displacement time history graphs of the node 5 for EFA and FBEA

EFA

FBEA

t=1.00 sec.

t=1.00 sec.

t=5.00 sec.

t=5.00 sec.

t=10.00 sec.

t=10.00 sec.

0.0   0.2   0.4   0.6   0.8   1.0
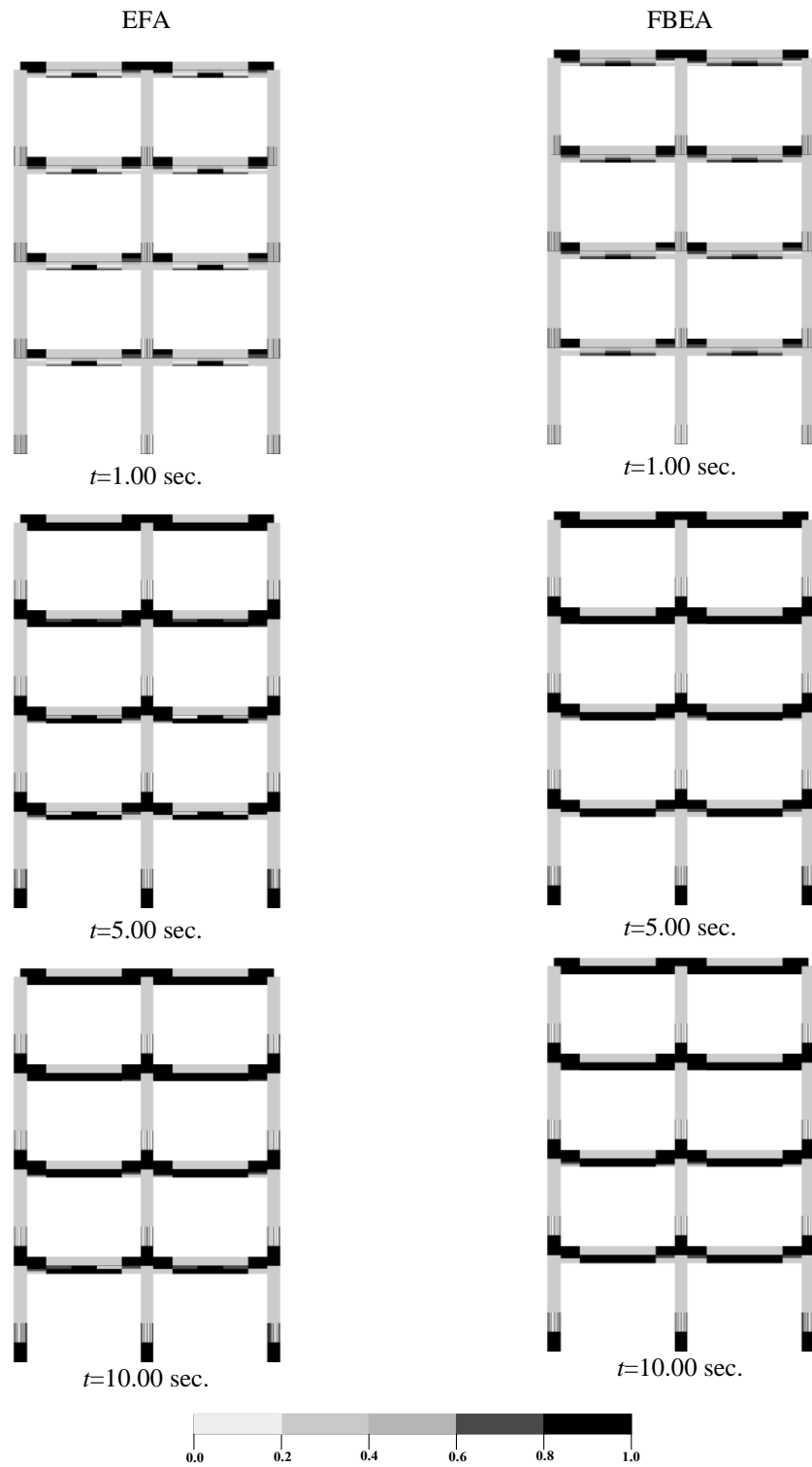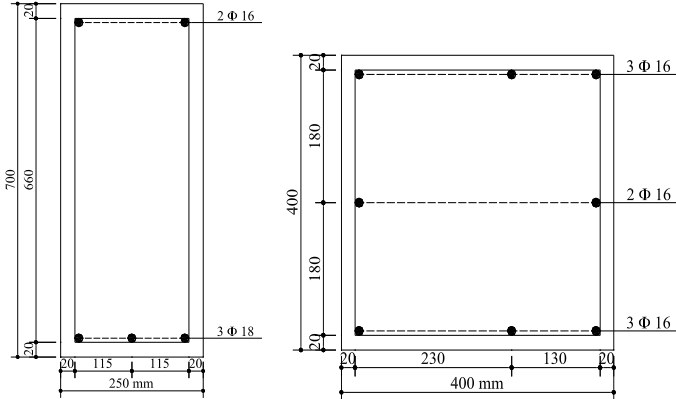
Fig. 7 Accumulated tensile damage zones of the 4-story frame according to EFA and FBEA

response differences for between both approaches are the result of reduction of shear strength due to damage in EFA.

Accumulated tensile damage cases obtained for both approaches are given in Fig. 7. Eq. (10) (Légeron *et al.* 2005) is used for the computation of tensile and compressive damages in both approaches. But compressive damages regions are not given due to small damaged/undamaged regions. Tensile damage zones for the EFA and FBEA are generally obtained at the upper parts of beams at the beam-column join region and at the lower parts of the mid region of the beams until the time=1.00 sec. Furthermore, an additional damage zone at lower parts of first-floor columns occurs for the both approach. Tensile damage intensities of beam obtained according to FBEA are some bigger than EFA. This case is clearly shown at time=5.0 sec. Damage intensities in beams and columns are some increased after this time. It is not seen a variety in the damage regions and an important increment in damage intensities until time=10.0 sec.

Accumulated tensile damage zone shapes and regions obtained from both approaches in columns are more similar. Some differences in damage regions of beams are obtained due to shear effect. Therefore, it might be said that some differentiations may be occurred for response quantities, damage regions and their intensities. But both approaches may be used for the numerical analysis of RC frames. However, a numerical dissipation for all solutions is not seen. Bossak-α integration with predicted-corrected method is successfully used for the nonlinear seismic analysis of RC frames.

Table 2 Material and cross section properties of 8-story RC frame

		Beam	Columns
Concrete	Elasticity Mod. (E_c MPa)	25742.960	25742.960
	Comp. strength (f_c, MPa)	30.00	30.00
	Tensile strength (f_t, MPa)	2.74	2.74
	Mass density (ρ, ton/m^3)	2.4	2.4
	Poisson ratio[*]	0.15	0.15
Steel	Elasticity Mod. (E_s MPa)	210000	210000
	Yield strength (f_y, MPa)	420.0	420.0
	Tangent modulus (α_t)	0.05	0.05
	Mass density (ρ, ton/m^3)	7.951	7.951
	Poisson ratio[*]	0.30	0.30

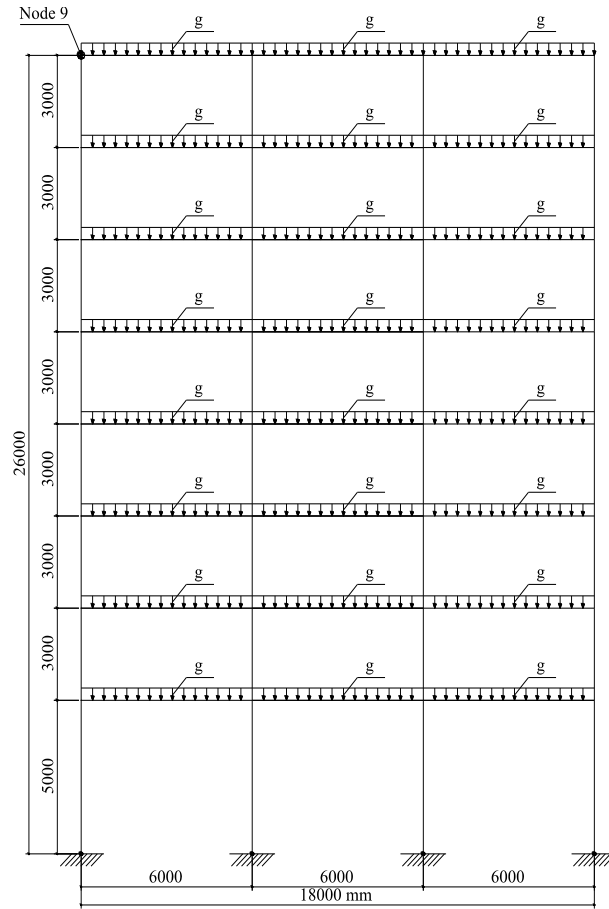[*]This material property is only used for EFA

Fig. 8 Finite element mesh of 8-story RC frame with soft-story

3.2 Nonlinear dynamic analyses of an 8-story RC frame structure with soft-story

In this numerical application, nonlinear seismic analyses of an 8-story RC frame structure with soft-story are obtained according to the both approaches. The material and section properties of the beam and column are given in Table 2 and the finite element mesh and loading case are also shown in Fig. 8. ACI 318-02 (2002) code is used for the material properties of concrete and steel. In this study, the same functions (Fig. 4) in the previous example for uniaxial stress-strain relationships for the concrete and reinforced bars in the EFA and FBEA are selected. Static loads and displacements are considered as the initial conditions. Element masses and loads of the beams are assumed to be distributed along to element length. The synthetic acceleration-time graph shown in Fig. 5 is used for the seismic analysis and it is the effect on the horizontal direction of the RC frame structure.

Horizontal (*x*) and vertical (*y*) displacement time history graphs of node 9 obtained from nonlinear dynamic analyses are shown in Fig. 9. Horizontal and vertical displacement time amplitude values are approximately similar until time 1.05 sec. Furthermore, a small phase difference appears between both methods after this time, this phase difference is clearly seen after

approximately time=5.5 sec. for both directions. Absolute maximum displacement values for vertical direction obtained from the EFA and the FBEA are 130.92 mm and 104.91 mm, respectively. Furthermore, absolute maximum displacement values for vertical direction obtained from the EFA and the FBEA are 3.15 mm and 3.01 mm, respectively. Displacement amplitude values of the EFA in horizontal and vertical directions are approximately 25% and 5% bigger than displacement values of the FBEA, respectively. These response differences of between both approaches are due to EFA, including shear damage.

Accumulated tensile damage cases obtained for both approaches are given in Fig. 10. But compressive damages regions are not given due to small damaged/undamaged regions. Tensile damage zones for EFA and FBEA are obtained at upper parts of the beams at beam-column join

(a) Horizontal

(b) Vertical
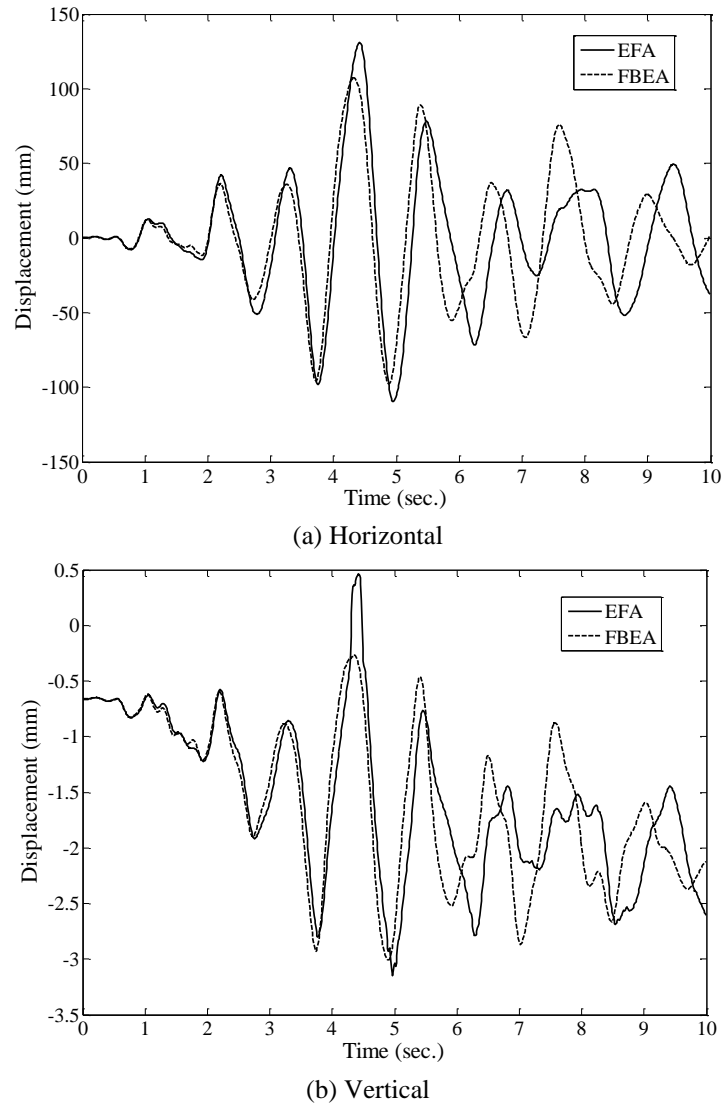
Fig. 9 Displacement time-history graphs of node 9 for EFA and FBEA

EFA

FBEA

t=1.00 sec.

t=1.00 sec.

t=5.00 sec.

t=5.00 sec.

t=10.00 sec.

t=10.00 sec.

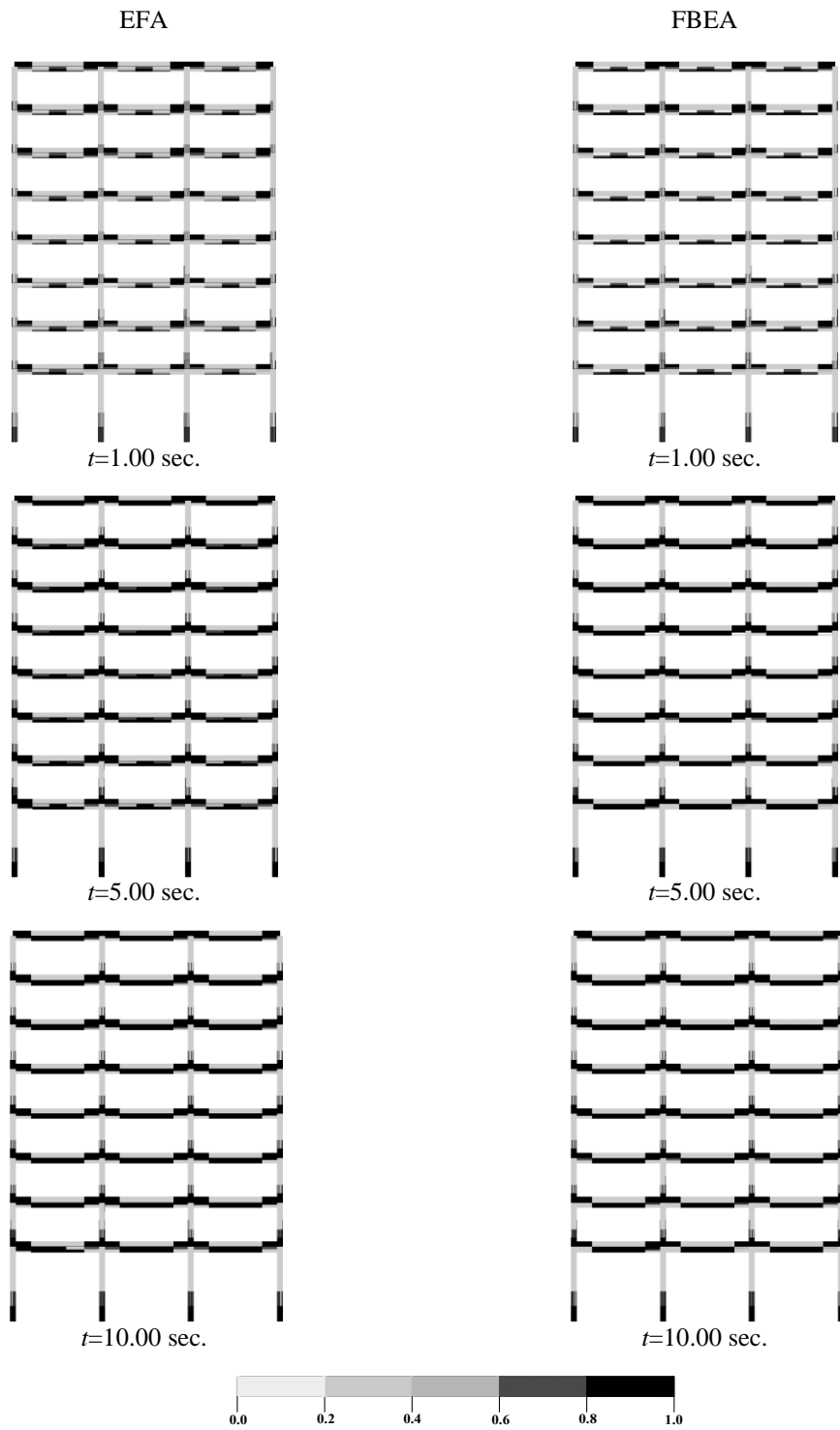| 0.0 | 0.2 | 0.4 | 0.6 | 0.8 | 1.0 |

Fig. 10 Accumulated tensile damage zones of the 8-story frame with soft-story for EFA and FBEA

regions and at the lower parts of the mid region of beams until the time=1.00 sec. Furthermore, an additional damage zone at lower parts of first-floor columns occurred for the both approaches. Tensile damage intensities in the beam obtained according to FBEA are some bigger than EFA. This case is shown clearly at time=5.0 sec. Later on, damage intensities in beams and columns increased. Accumulated damage zone shapes and regions obtained from both approaches are generally more similar. Therefore, it might be said that some differentiations that may occur for response quantities, damage regions and their intensities and numerical dissipation are not seen for all solutions; both approaches may be used for the numerical analysis of RC frames. But shear effect should be included for nonlinear dynamic analysis of the frames.

4. Conclusions

In this study, two beam-column elements based on the Elasto-Fiber element theory for reinforced concrete (RC) element have been developed and compared with each other. The first element is based on Elasto Fiber Approach (EFA) was initially developed for steel structures and this theory was applied for RC element in there. And the second element is called as Fiber&Bernoulli-Euler element approach (FBEA). In this element, Cubic Hermitian polynomials are used for obtaining stiffness matrix. The beams or columns element in both approaches are divided into a sub-element called the segment for obtaining element stiffness matrix. The internal freedoms of this segment are dynamically condensed to the external freedoms at the ends of the element by using a dynamic substructure technique. Thus, nonlinear dynamic analysis of high RC building can be obtained within short times. In addition to, external loads of the segment are assumed to be distributed along to element. Therefore, damages can be taken account of along to element and redistributions of the loading for solutions. Bossak-α integration with predicted-corrected method is used for the nonlinear seismic analysis of RC frames. For numerical application, seismic damage analyses for a 4-story frame and an 8-story RC frame with soft-story are obtained to comparisons of RC element according to both approaches. Damages evaluation and propagation in the frame elements are studied and response quantities from obtained both approaches are investigated in the detail.

In the response quantities, absolute amplitude values of displacement of the EFA in horizontal and vertical directions of top nodes of both frames are generally bigger than displacement values of the FBEA. These response differences between both approaches are due to EFA including shear damage.

Accumulated tensile damage regions obtained for both approaches are observed at upper parts of the beams at the beam-column join regions and at the lower parts of the mid region of the beams; an additional damage zone at lower parts of first-floor columns occurs for the both approaches. Damage intensities in the beam especially obtained from FBEA are some bigger than EFA. These differences between both approaches are due to EFA including shear damage. Accumulated damage zone shapes and regions obtained from both approaches are generally more similar. But EFA must be preferred for more realistic results.

Therefore, it might be said that some differentiations may occur for response quantities, damage regions and their intensities. Numerical dissipation of all solutions is not seen and Bossak-α integration with predicted-corrected method can be used for the nonlinear seismic analysis of RC frames

References

Anagnostoupoulos, S. (1981), "Inelastic beams for seismic analysis of structures", *J. Eng. Mech.*, **107**(ST7), 1297-1311.

ACI 318-02 (2002), *Building code requirements for Structural concrete*, American Concrete Institute, USA.

Banon H., Biggs, J. and Irvine, M. (1981), "Seismic damage in reinforced concrete frames", *J. Struct. Eng.*, **107**(ST9), 1713-1729.

Bathe, K.J. (1982), *Finite Element Procedures in Engineering Analysis*, Prentice Hall, Englewood Cliffs, New Jersey, USA.

Carlson, A.E. (1999), "Three-dimensional nonlinear inelastic analysis of steel moment-frame buildings damaged by earthquake excitations", EERL Report 1999/02, Earthquake Engineering Research Laboratory, Berkeley, California.

Ceresa, P., Petrini, L. Pinho, R. and Sousa, R. (2009), "A fibre flexure-shear model for seismic analysis of RC-framed structures", *Earthq. Eng. Struc. Dyn.*, **38**(5), 565-586.

Chandrupatla, T.R. and Belegundu, A.D. (2002), *Introduction to Finite Elements in Engineering*, Prentice Hall, Upper Saddle River, NJ, USA.

Filippou, F.C. and Issa, A. (1988), "Nonlinear analysis of reinforced concrete frames under cyclic load reversals", EERC Report 1988/12, Earthquake Engineering Research Laboratory, Berkeley, California.

Guyan, R.J. (1965), "Reduction of stiffness and mass matrices", *AIAA J.*, **3**(2), 380.

http://opensees.berkeley.edu, Open System for Earthquake Engineering Simulation, OpenSees, Pacific Earthquake Engineering Research Center, University of California, Berkeley.

http://www.seismosoft.com, SeismoArtif Ver 1.

Iribarren, B.S. (2010), "Progressive collapse simulation of reinforced concrete structures: influence of design and material parameters and investigation of the strain rate effects", Ph.D. Thesis, Polytechnic Faculty, Faculty of Applied Sciences, Bruxelles Royal Military Academy, Université Libre de.

Isobe, D. and Tsuda, M. (2003), "Seismic collapse analysis of reinforced concrete framed structures using the finite element method", *Earthq. Eng. Struct. Dyn.*, **32**(13), 2027-2046.

Kawano, A., Griffith, M.C., Joshi, H.R. and Warner, R.F. (1998), "Analysis of behaviour and collapse of concrete frames subjected to severe ground motion", Department of Civil and Environmental Engineering, R163, Adelaide University, South Australia.

Karaton, M. (2013), "Nonlinear earthquake analysis of reinforced concrete frames with fiber and Bernoulli-Euler Beam-Column element", *Sci. World J.*, Article ID 905963, 15.

Krishnan, S. (2003), "Three-dimensional nonlinear analysis of tall irregular steel buildings subject to strong ground motion", EERL Report 2003/01, Earthquake Engineering Research Laboratory, Berkeley, California.

Légeron, F., Paultre, P. and Mazars, J. (2005), "Damage mechanics modeling of nonlinear seismic behaviour of concrete structures", *J. Struct. Eng.*, **131**(6), 946-954.

Li, Y., Lu, X.Z., Guan, H. and Ye, L.P. (2011), "An improved tie force method for progressive collapse resistance design of reinforced concrete frame structures", *Eng. Struct.*, **33**(10), 2931-2942.

Lu, X., Lu, X., Guan, H. and Ye, l. (2013), "Collapse simulation of reinforced concrete high-rise building induced by extreme earthquakes", *Earthq. Eng. Struct. Dyn.*, **42**(5), 705-723.

Miranda, I., Ferencz, R.M. and Hughes, T.J.R. (1989), "An improved implicit-explicit time integration method for structural dynamics", *Earthq. Eng. Struct. Dyn.*, **18**(5), 643-653.

Taucer, F.F., Spacone, E. and Filippou, F.C. (1991), "A fibre beam-column element for seismic response analysis of reinforced concrete structures", EERC 1991/17, Earthquake Engineering Research Center, Berkeley, California.

TRBDA (2007), *Turkish Regulation on Building in Disaster Area*, Ankara, Turkey. (in Turkish)

Wood, W.L., Bossak, M. and Zienkiewicz, O.C. (1980), "A alpha modification of Newmark's method", *Int. J. Numer. Meth. Eng.*, **15**(10), 1562-1566.

Lu, X., Lu, X.Z., Guan, H. and Ye, L. (2013), "Collapse simulation of reinforced concrete high-rise building

induced by extreme earthquakes", *Earth.Eng.&Struc.Dyn.*, **42**(5), 705-723.
Zeris, C. and Mahin, S. (1991), "Behavior of reinforced concrete structures subjected to biaxial excitation",
    J. Struct. Eng., **117**(ST9), 2657-2673.

Appendix

Time marching algorithm

The algorithm applied to Eq. (26) is as follows
1. Compute integration parameters

$$A_1 = \frac{1}{\beta \Delta t^2} \; ; \qquad A_2 = \frac{\gamma}{\beta \Delta t} \tag{30}$$

2. $\{u_S\}_{t+\Delta t}$, $\{v_S\}_{t+\Delta t}$ and $\{a_S\}_{t+\Delta t}$ are known; set global iteration counter, $i=1$.
3. Predict response at $t+\Delta t$

$$\{u_S\}_{t+\Delta t}^i = \{\tilde{u}_S\}_{t+\Delta t} \tag{31a}$$

$$\{v_S\}_{t+\Delta t}^i = \{\tilde{v}_S\}_{t+\Delta t} \tag{31b}$$

$$\{a_S\}_{t+\Delta t}^i = \{0\} \tag{31c}$$

4. Set element counter, *nel*=1
5. Set element iteration counter, *j*=1.
   Subtract incremental displacement vector of external joints from global displacement vectors

$$\{\Delta u_E\}_{t+\Delta t}^j = SUB\left(\{\Delta u_S\}_{t+\Delta t}^i\right) \tag{32}$$

6. Compute the element stiffness, mass, damping matrices and element external and internal force vectors,
7. Compute iterative and incremental displacement vectors of internal joints

$$\{\Delta u_I\}_{t+\Delta t}^{j+1} = [K_{II}]_{t+\Delta t}^j \left(\left(\{\Delta F_{I,gr}\}_{t+\Delta t}^{j+1} - \{\Delta F_{I,res}\}_{t+\Delta t}^{j+1}\right) - [K_{IE}]_{t+\Delta t}^j \{\Delta u_E\}_{t+\Delta t}^i\right) \tag{33.a}$$

$$\{u_I\}_{t+\Delta t}^{j+1} = \{u_I\}_{t+\Delta t}^j + \{\Delta u_I\}_{t+\Delta t}^{j+1} \tag{33.b}$$

8. Check for convergence of iteration process $\left\|\{\Delta u_I\}_{t+\Delta t}^{j+1}\right\|$ (Euclidian norm of the unbalanced internal displacement vector at time step $t+\Delta t$ and element iteration *j*) using an element displacement tolerance (*Tolelem*).

a) If $\left\|\{\Delta u_I\}_{t+\Delta t}^{j+1}\right\| \bigg/ \left\|\sum_{m=1}^{j+1}\{\Delta u_I\}_{t+\Delta t}^m\right\| \leq Tolelem$, convergence is achieved.

Set

$$\{u_I\}_t = \{u_I\}_{t+\Delta t}^{j+1}, \quad \{v_I\}_t = \{v_I\}_{t+\Delta t}^{j+1} \text{ and } \{a_I\}_t = \{a_I\}_{t+\Delta t}^{j+1} \tag{34a}$$

$$\left[K_{EE,F}\right]_{t+\Delta t}^{j} = \left[K_{EE}\right]_{t+\Delta t}^{j} - \left[K_{EI}\right]_{t+\Delta t}^{j} \left(\left[K_{II}\right]_{t+\Delta t}^{j}\right)^{-1} \left[K_{IE}\right]_{t+\Delta t}^{j} \tag{34b}$$

$$\left\{F_{E,F}\right\}_{t+\Delta t}^{i+1} = \left\{F_{E}\right\}_{t+\Delta t}^{j+1} - \left[K_{EI}\right]_{t+\Delta t}^{j} \left(\left[K_{II}\right]_{t+\Delta t}^{j}\right)^{-1} \left\{F_{I}\right\}_{t+\Delta t}^{j+1} \tag{34c}$$

$$\left[M_{EE,F}\right]_{t+\Delta t}^{j} = \left[M_{EE}\right]_{t+\Delta t}^{j} - \left[K_{EI}\right]_{t+\Delta t}^{j} \left(\left[K_{II}\right]_{t+\Delta t}^{j}\right)^{-1} \left[M_{IE}\right]_{t+\Delta t}^{j}$$

$$\qquad - \left[M_{EI}\right]_{t+\Delta t}^{j} \left(\left[K_{II}\right]_{t+\Delta t}^{j}\right)^{-1} \left[K_{IE}\right]_{t+\Delta t}^{j} \tag{34d}$$

$$\qquad + \left[K_{EI}\right]_{t+\Delta t}^{j} \left(\left[K_{II}\right]_{t+\Delta t}^{j}\right)^{-1} \left[M_{II}\right]_{t+\Delta t}^{j} \left(\left[K_{II}\right]_{t+\Delta t}^{j}\right)^{-1} \left[K_{IE}\right]_{t+\Delta t}^{j}$$

$$\left[C_{EE,F}\right]_{t+\Delta t}^{j} = \left[C_{EE}\right]_{t+\Delta t}^{j} - \left[K_{EI}\right]_{t+\Delta t}^{j} \left(\left[K_{II}\right]_{t+\Delta t}^{j}\right)^{-1} \left[C_{IE}\right]_{t+\Delta t}^{j}$$

$$\qquad - \left[C_{EI}\right]_{t+\Delta t}^{j} \left(\left[K_{II}\right]_{t+\Delta t}^{j}\right)^{-1} \left[K_{IE}\right]_{t+\Delta t}^{j} \tag{34e}$$

$$\qquad + \left[C_{EI}\right]_{t+\Delta t}^{j} \left(\left[K_{II}\right]_{t+\Delta t}^{j}\right)^{-1} \left[C_{II}\right]_{t+\Delta t}^{j} \left(\left[K_{II}\right]_{t+\Delta t}^{j}\right)^{-1} \left[K_{IE}\right]_{t+\Delta t}^{j}$$

$$\left[K_{S}\right] = \sum_{k=1}^{nelem} \left[K_{EE,F}\right]_{t+\Delta t}^{j}, \quad \left[C_{S}\right] = \sum_{k=1}^{nelem} \left[C_{EE,F}\right]_{t+\Delta t}^{j}$$

$$\left[M_{S}\right] = \sum_{k=1}^{nelem} \left[M_{EE,F}\right]_{t+\Delta t}^{j}, \quad \left\{F_{S}\right\} = \sum_{k=1}^{nelem} \left\{F_{E,F}\right\}_{t+\Delta t}^{j} \tag{34f}$$

    b) If global convergence is not achieved; set $j=j+1$ and return to step 5.

9. Compute the effective dynamic stiffness matrix and the vector of unbalanced forces

$$\left[\hat{K}_{S}\right]_{t+\Delta t}^{i} = (1-\alpha_{B})A_{I}\left[M_{S}\right] + A_{2}\left[C_{S}\right]_{t+\Delta t} + \left[K_{S}\right]_{t+\Delta t} \tag{35.a}$$

$$\left\{\Delta F_{S}\right\}_{t+\Delta t}^{i+1} = (1-\alpha_{B})\left\{F_{S}\right\}_{t+\Delta t} + \alpha_{B}\left\{F_{S,gr}\right\}_{t} - \left\{\Delta F_{S,res}\right\}_{t+\Delta t}^{i+1} + \left\{F_{S,stat}\right\}$$

$$\qquad + \left[M_{S}\right]\left(-(1-\alpha_{B})\left\{a_{S}\right\}_{t+\Delta t}^{i+1} + \alpha_{B}\left\{a_{S}\right\}_{t}^{i}\right) - \left[C_{S}\right]_{t+\Delta t}^{i}\left\{v_{S}\right\}_{t+\Delta t}^{i+1} \tag{35.b}$$

where $\left[K_{S}\right]_{t+\Delta t}^{i}$ and $\left\{\Delta F_{S,res}\right\}_{t+\Delta t}^{i+1}$ are the tangent stiffness matrix and the incremental restoring force vector of external joints on the global axis of the structure, respectively, which are assembled from the element contributions.

10. Solve for incremental displacements in the global axis

$$\left[\hat{K}_{S}\right]_{t+\Delta t}^{i}\left\{\Delta u_{S}\right\}_{t+\Delta t}^{i+1} = \left\{\Delta F_{S}\right\}_{t+\Delta t}^{i+1} \tag{36}$$

11. Update displacement, velocity and acceleration vectors

$$\left\{u_{S}\right\}_{t+\Delta t}^{i+1} = \left\{u_{S}\right\}_{t+\Delta t}^{i} + \left\{\Delta u_{S}\right\}_{t+\Delta t}^{i+1} \tag{37.a}$$

$$\left\{ v_S \right\}_{t+\varDelta t}^{i+1} = \left\{ \tilde{v}_S \right\}_{t+\varDelta t} + A_2 \left(\left\{ u_S \right\}_{t+\varDelta t}^{i+1} - \left\{ \tilde{u}_S \right\}_{t+\varDelta t} \right) \tag{37.b}$$

$$\left\{ a_S \right\}_{t+\varDelta t}^{i+1} = A_1 \left(\left\{ u_S \right\}_{t+\varDelta t}^{i} - \left\{ \tilde{u}_S \right\}_{t+\varDelta t} \right) \tag{37.c}$$

12. Check for convergence of the iteration process $\left\| \left\{ \varDelta F_S \right\}_{t+\varDelta t}^{i+1} \right\|$ (Euclidian norm of the unbalanced force vector at time step $t+\varDelta t$ and global iteration i) using a force tolerance (*Tolglo*).

a)   If $\left\| \left\{ \varDelta F_E \right\}_{t+\varDelta t}^{i+1} \right\| \Big/ \left\| \sum_{n=1}^{i+1} \left\{ \varDelta F_E \right\}_{t+\varDelta t}^{n} \right\| \le To \lg lo$, convergence is achieved.

Set $\left\{ u_S \right\}_t = \left\{ u_S \right\}_{t+\varDelta t}^{i+1}$, $\left\{ v_S \right\}_t = \left\{ v_S \right\}_{t+\varDelta t}^{i+1}$ and $\left\{ a_S \right\}_t = \left\{ a_S \right\}_{t+\varDelta t}^{i+1}$

b)   If global convergence is not achieved; set $i=i+1$ and return to step 4.

13. Set $t=t+\Delta t$ and return step to 2.